Earthline Journal of Mathematical Sciences
E-ISSN: 2581-8147
Volume 16, Number 6, November 2026, Pages 1245-1265
https://doi.org/10.34198/ejms.16626.78.12451265

The New Arctangent-Tangent Distribution: Theory, Simulations, and Practice

Festus C. Opone[1], Christophe Chesneau[2] and Francis E. Itiveh[3]

[1] Department of Statistics, Southern Delta University, Ozoro, Nigeria
e-mail: oponef@sdu.edu.ng

[2] Department of Mathematics, LMNO, University of Caen, 14032 Caen, France
e-mail: christophe.chesneau@gmail.com

[3] Department of Statistics, Southern Delta University, Ozoro, Nigeria
e-mail: itivehfe@sdu.edu.ng

Abstract

This article introduces a novel unit distribution, referred to as the new arctangent-tangent (NAT) distribution. Its fundamental properties are derived, with particular emphasis on the cumulative distribution function, probability density function, and quantile function. Building on this framework, the NAT distribution is further extended to construct a new lifetime distribution, termed the new arctangent-tangent-exponential (NAT-E) distribution. The key properties of this extended distribution are similarly investigated, with a focus on its distributional characteristics and analytical tractability. We introduce five parameter-estimation methods and conduct a Monte Carlo simulation to examine the asymptotic behaviour of the estimators. Finally, the proposed models are applied to real data, where they demonstrate superior performance compared to a certain number of standard models commonly used in the literature.

1 Introduction

Unit distributions are defined by their support on the interval $(0, 1)$. These distributions are foundational in probability and statistics due to their capacity to represent proportions, rates, and fractional data. Beyond direct modeling, they serve as versatile generators for broader families of distributions across various supports. For a comprehensive overview of this field, we refer to the exhaustive 2025 survey by [1]; several specific unit distributions from this literature are discussed later in this study. Building on these developments, [3] introduced a novel unit distribution, called the arctangent-tangent (AT) distribution, defined by the following cumulative distribution function (CDF):

$$F(x) = \frac{2}{\pi} \arctan\left(\left(\tan\left(\frac{\pi}{2}x\right)\right)^{\alpha}\right), \quad x \in (0,1), \tag{1}$$

Received: September 6, 2026; Revised & Accepted: November 10, 2026; Published online: November 13, 2026
2020 Mathematics Subject Classification: 60E05, 62E10.
Keywords and phrases: unit distribution, NAT distribution, estimation methods, simulation experiment.
*Corresponding author
Copyright 2026 the Authors

where $\alpha > 0$ is a shape parameter. Notably, when $\alpha = 1$, the model simplifies to the classical continuous uniform distribution on $(0, 1)$. For $\alpha \neq 1$, the distribution offers new modeling perspectives, providing the flexibility to capture various data behaviors within the unit interval.
The aim of this article is threefold:

1. We propose an extension of the AT distribution, called the new arctangent-tangent (NAT) distribution by introducing an adjustable parameter β within the primary arctangent term. We demonstrate that the resulting function remains a valid CDF. Furthermore, we derive its fundamental properties, including the probability density function (PDF) and quantile function (QF), highlighting their analytical tractability

2. Building upon the NAT distribution, which allows for the generation of distributions with various supports, we introduce another flexible three-parameter lifetime distribution referred to as the new arctangent-tangent-exponential(NAT-E) distribution. We derive its fundamental properties, specifically the CDF, PDF, and QF, while emphasizing their analytical tractability.

3. While applications are not addressed in [3], the present study evaluates the practical utility of the new models through a comprehensive data analysis. By examining three distinct datasets, we demonstrate that these models can outperform several standard benchmarks found in the literature.

The remainder of this article is organized as follows: Section 2 introduces and investigates the properties of the new unit distribution. In Section 3, the derived lifetime distribution is presented, and its characteristics are studied. In Section 4, five methods of parameter estimation are studied, while the asymptotic behaviour of the unknown parameters of the NAT-E distribution is examined in Section 5. Section 6 is dedicated to practical applications, while Section 7 provides concluding remarks.

2 A New Unit Distribution

The theorem below presents an extended CDF based on the AT distribution in Equation (1). Its main contribution is the addition of the parameter β at a specific location to enhance flexibility.

Theorem 2.1. *The following function is a valid CDF of a unit distribution:*

$$F(x) = \frac{2}{\pi} \arctan\left(\beta \left(\tan\left(\frac{\pi}{2}x\right)\right)^{\alpha}\right), \quad x \in (0, 1),$$

with $\alpha > 0$ and $\beta > 0$, and is completed by setting $F(x) = 0$ for any $x \leq 0$ and $F(x) = 1$ for any $x \geq 1$.

Proof. The continuity of F is immediate on $\mathbb{R}\backslash\{0, 1\}$. Let us investigate this continuity at the points 0 and 1. For the point 0, the following holds:

$$\lim_{x \to 0^+} \tan\left(\frac{\pi}{2}x\right) = 0,$$

so that

$$\lim_{x\to 0^+} \beta\left(\tan\left(\frac{\pi}{2}x\right)\right)^{\alpha} = 0,$$

and

$$\lim_{x\to 0^+} F(x) = \lim_{x\to 0^+} \frac{2}{\pi}\arctan\left(\beta\left(\tan\left(\frac{\pi}{2}x\right)\right)^{\alpha}\right) = 0 = F(0).$$

F is thus continuous at the point 0.

For the point 1, we proceed similarly. We have

$$\lim_{x\to 1^-} \tan\left(\frac{\pi}{2}x\right) = +\infty,$$

so that

$$\lim_{x\to 1^-} \beta\left(\tan\left(\frac{\pi}{2}x\right)\right)^{\alpha} = +\infty,$$

and

$$\lim_{x\to 1^-} F(x) = \lim_{x\to 1^-} \frac{2}{\pi}\arctan\left(\beta\left(\tan\left(\frac{\pi}{2}x\right)\right)^{\alpha}\right) = \frac{2}{\pi}\times\frac{\pi}{2} = 1 = F(1).$$

F is thus continuous at 1. This completes the proof of the full continuity of F on $\mathbb{R}$.

Using standard derivation techniques, for any $x \in (0,1)$, we have

$$F'(x) = \alpha\beta\frac{\left(\tan\left((\pi/2)x\right)\right)^{\alpha-1}}{\left(\cos\left((\pi/2)x\right)\right)^2\left(1+\beta^2\left(\tan\left((\pi/2)x\right)\right)^{2\alpha}\right)}.$$

It is clear that $F'(x) \geq 0$, implying that F is increasing. We also obviously have $F(x) \in [0,1]$ for any $x \in \mathbb{R}$. As a result, F is a valid CDF of a unit distribution. This concludes the proof. □

We call the unit distribution defined by the CDF F given in Theorem 2.1 the NAT distribution. If we take $\beta = 1$, it is reduced to the AT distribution.

For illustrative purposes, Figure 1 presents the curves of F for several values of α and β.

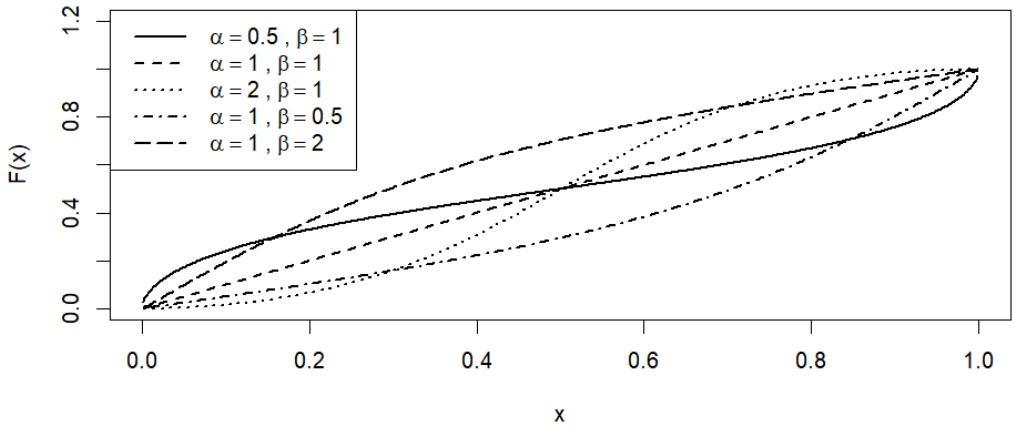


Figure 1: Curves of the CDF of the NAT distribution for several values of α and β.

Various concave and convex shapes are observed, illustrating the significant structural flexibility of the NAT distribution.

The PDF associated with the NAT distribution is a part of the proof of Theorem 2.1; it is given by

$$f(x) = \alpha\beta \frac{(\tan((\pi/2)x))^{\alpha-1}}{(\cos((\pi/2)x))^2 \left(1+\beta^2 (\tan((\pi/2)x))^{2\alpha}\right)}, \quad x \in (0,1),$$

and is completed by setting $f(x) = 0$ for any $x \notin (0,1)$. For illustrative purposes, Figure 2 presents the curves of f for several values of α and β.

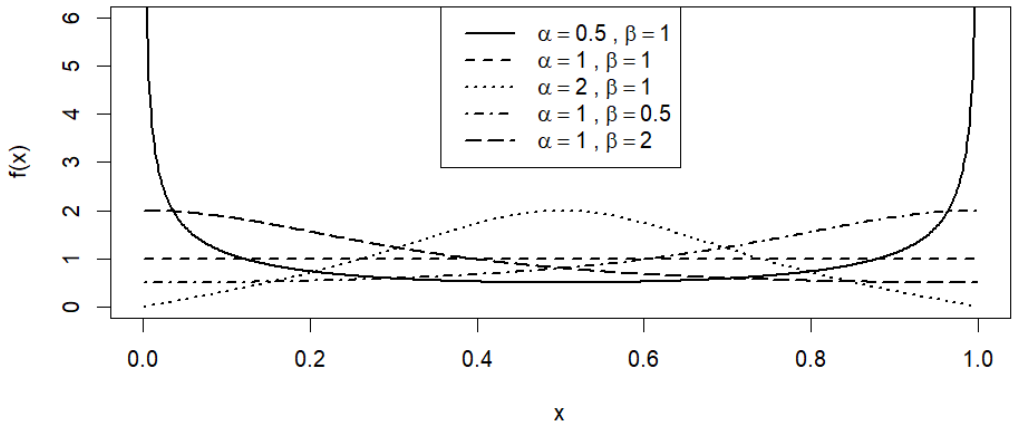


Figure 2: Curves of the PDF of the NAT distribution for several values of α and β.

The distribution exhibits a wide range of profiles, including bathtub-shaped, decreasing, increasing, and unimodal forms. Furthermore, the PDF can take on both symmetric and asymmetric shapes, further demonstrating the structural flexibility of the NAT distribution.

We end this analysis by the QF associated with the NAT distribution, which is presented below.

Theorem 2.2. *The QF associated with the NAT distribution is given by*

$$Q(u) = \frac{2}{\pi} \arctan\left(\left(\frac{1}{\beta}\tan\left(\frac{\pi}{2}u\right)\right)^{1/\alpha}\right), \quad u \in (0,1),$$

with $\alpha > 0$ *and* $\beta > 0$.

Proof. The QF associated with the NAT distribution is the inverse function of the CDF F, as described in Theorem 2.1. Therefore, we need to solve the equation $F(x) = u$. This yields the following equivalences:

$$\frac{2}{\pi}\arctan\left(\beta\left(\tan\left(\frac{\pi}{2}x\right)\right)^{\alpha}\right) = u \;\Leftrightarrow\; \beta\left(\tan\left(\frac{\pi}{2}x\right)\right)^{\alpha} = \tan\left(\frac{\pi}{2}u\right)$$
$$\Leftrightarrow\; \tan\left(\frac{\pi}{2}x\right) = \left(\frac{1}{\beta}\tan\left(\frac{\pi}{2}u\right)\right)^{1/\alpha} \;\Leftrightarrow\; x = \frac{2}{\pi}\arctan\left(\left(\frac{1}{\beta}\tan\left(\frac{\pi}{2}u\right)\right)^{1/\alpha}\right).$$

Therefore, we have

$$Q(u) = \frac{2}{\pi} \arctan\left(\left(\frac{1}{\beta}\tan\left(\frac{\pi}{2}u\right)\right)^{1/\alpha}\right), \quad u \in (0,1).$$

This completes the proof. □

In summary, we have introduced a new unit distribution, the NAT distribution, which features analytically tractable expressions for its core probabilistic functions. Its CDF and PDF exhibit significant flexibility, accommodating a wide variety of shapes. The empirical utility of the NAT distribution will be further explored through data analysis in Section 6.

In the subsequent section, we use the NAT distribution to develop a new three-parameter lifetime model, termed the NAT-E distribution.

3 The NAT-E Distribution

Let G be a CDF of a continuous distribution. Then, based on the NAT distribution, we define a new CDF by the following composition function:

$$H(x) = F(G(x)), \quad x \in \mathbb{R}.$$

In particular, by considering the CDF of an exponential distribution with parameter λ for $G(x)$, i.e., $G(x) = 1 - e^{-\lambda x}$ for any $x \geq 0$, which we complete by setting $G(x) = 0$ for any $x < 0$, we define the

NAT-E distribution by the following CDF:

$$H(x) = \frac{2}{\pi} \arctan\left(\beta \left(\tan\left(\frac{\pi}{2}(1 - e^{-\lambda x})\right)\right)^{\alpha}\right), \quad x \geq 0, \tag{2}$$

with $\alpha > 0$, $\beta > 0$ and $\lambda > 0$, and is completed by setting $H(x) = 0$ for any $x < 0$.

Using the formula $\tan((\pi/2)(1-y)) = 1/\tan((\pi/2)y)$, it can also be written as

$$H(x) = \frac{2}{\pi} \arctan\left(\beta \left(\tan\left(\frac{\pi}{2} e^{-\lambda x}\right)\right)^{-\alpha}\right), \quad x \geq 0,$$

with $\alpha > 0$, $\beta > 0$ and $\lambda > 0$, and is completed by setting $H(x) = 0$ for any $x \leq 0$. For illustrative purposes, Figure 3 presents the curves of H for several values of α, β and λ.

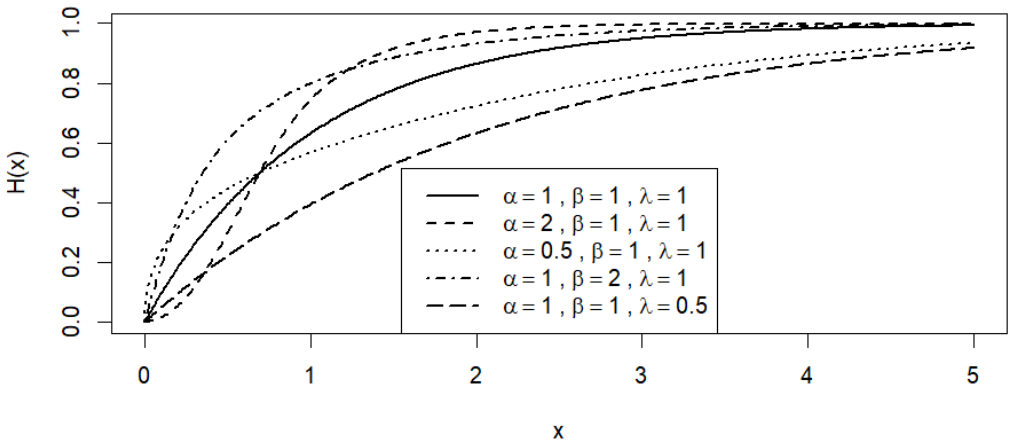


Figure 3: Curves of the CDF of the NAT-E distribution for several values of α, β and λ.

The distribution exhibits various increasing concave forms, further illustrating the structural flexibility of the NAT-E distribution.

The PDF associated with the NAT-E distribution is obtained by derivation of H, which gives

$$h(x) = \alpha\beta\lambda \frac{e^{-\lambda x}\left(\tan\left((\pi/2)e^{-\lambda x}\right)\right)^{-(\alpha-1)}}{\left(\sin\left((\pi/2)e^{-\lambda x}\right)\right)^2 \left(1 + \beta^2 \left(\tan\left((\pi/2)e^{-\lambda x}\right)\right)^{-2\alpha}\right)}, \quad x \geq 0, \tag{3}$$

and is completed by setting $h(x) = 0$ for any $x < 0$. For illustrative purposes, Figure 4 presents the curves of h for several values of α, β and λ.

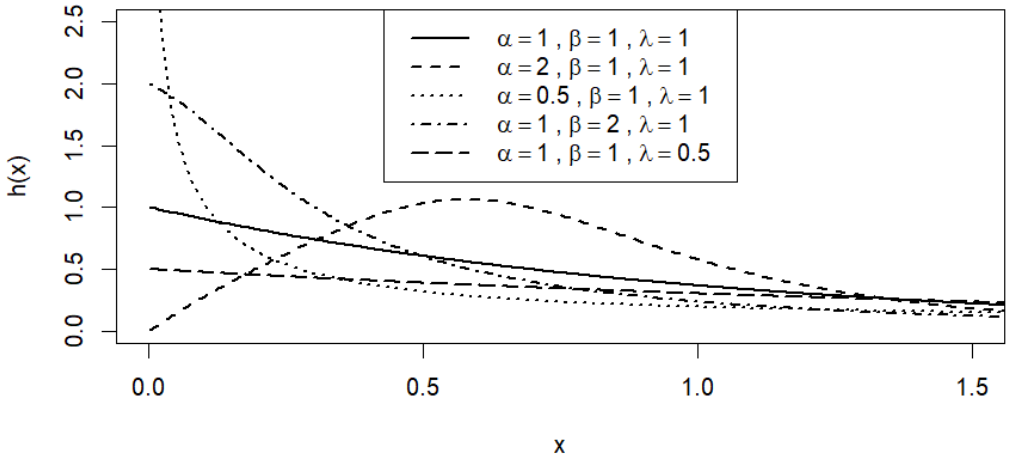


Figure 4: Curves of the PDF of the NAT-E distribution for several values of α, β and λ.

The distribution exhibits a wide range of profiles, including monotonic decreasing and unimodal shapes. Furthermore, the capacity to accommodate both symmetric and asymmetric forms highlights the versatility of the NAT-E model for diverse lifetime data analyses.

The survival and hazard rate functions of the NAT-E distribution can further be derived, respectively, as

$$S(x) = 1 - \frac{2}{\pi} \arctan\left(\beta \left(\tan\left(\frac{\pi}{2} e^{-\lambda x}\right)\right)^{-\alpha}\right), \quad x \geq 0,$$

and completed by setting $S(x) = 1$ for $x < 0$, and

$$j(x) = \alpha\beta\lambda \frac{e^{-\lambda x}\left(\tan\left((\pi/2)e^{-\lambda x}\right)\right)^{-(\alpha-1)}\left[1 - (2/\pi)\arctan\left(\beta\left(\tan\left((\pi/2)e^{-\lambda x}\right)\right)^{-\alpha}\right)\right]}{\left(\sin\left((\pi/2)e^{-\lambda x}\right)\right)^{2}\left(1 + \beta^2\left(\tan\left((\pi/2)e^{-\lambda x}\right)\right)^{-2\alpha}\right)}, \quad x \geq 0,$$

and completed by setting $j(x) = 0$ for $x < 0$. We end this analysis with the QF associated with the NAT-E distribution, which is described below.

Theorem 3.1. *The QF associated with the NAT-E distribution is given by*

$$K(u) = -\frac{1}{\lambda} \log\left(1 - \frac{2}{\pi} \arctan\left(\left(\frac{1}{\beta} \tan\left(\frac{\pi}{2} u\right)\right)^{1/\alpha}\right)\right), \quad u \in (0, 1), \tag{4}$$

with $\alpha > 0$, $\beta > 0$ and $\lambda > 0$.

Proof. The QF associated with the NAT-E distribution is the inverse function of the CDF H, as described in Equation (2). Therefore, we need to solve the equation $H(x) = u$. This yields the following equivalences:

$$\begin{aligned}
&\frac{2}{\pi}\arctan\left(\beta\left(\tan\left(\frac{\pi}{2}(1-e^{-\lambda x})\right)\right)^{\alpha}\right) = u \;\Leftrightarrow\; \beta\left(\tan\left(\frac{\pi}{2}(1-e^{-\lambda x})\right)\right)^{\alpha} = \tan\left(\frac{\pi}{2}u\right)\\
&\Leftrightarrow\; \tan\left(\frac{\pi}{2}(1-e^{-\lambda x})\right) = \left(\frac{1}{\beta}\tan\left(\frac{\pi}{2}u\right)\right)^{1/\alpha} \;\Leftrightarrow\; 1-e^{-\lambda x} = \frac{2}{\pi}\arctan\left(\left(\frac{1}{\beta}\tan\left(\frac{\pi}{2}u\right)\right)^{1/\alpha}\right)\\
&\Leftrightarrow\; e^{-\lambda x} = 1-\frac{2}{\pi}\arctan\left(\left(\frac{1}{\beta}\tan\left(\frac{\pi}{2}u\right)\right)^{1/\alpha}\right)\\
&\Leftrightarrow\; x = -\frac{1}{\lambda}\log\left(1-\frac{2}{\pi}\arctan\left(\left(\frac{1}{\beta}\tan\left(\frac{\pi}{2}u\right)\right)^{1/\alpha}\right)\right).
\end{aligned}$$

Therefore, we have

$$K(u) = -\frac{1}{\lambda}\log\left(1-\frac{2}{\pi}\arctan\left(\left(\frac{1}{\beta}\tan\left(\frac{\pi}{2}u\right)\right)^{1/\alpha}\right)\right), \quad u\in(0,1).$$

This completes the proof. □

By inserting $u = 0.5$ into Equation (4), the median of the NAT-E distribution is derived as

$$K(0.5) = -\frac{1}{\lambda}\log\left(1-\frac{2}{\pi}\arctan\left(\left(\frac{1}{\beta}\tan\left(\frac{\pi}{4}\right)\right)^{1/\alpha}\right)\right).$$

Other measures of partition, including the lower and upper quartiles, are obtained, respectively, as

$$K\left(\frac{1}{4}\right) = -\frac{1}{\lambda}\log\left(1-\frac{2}{\pi}\arctan\left(\left(\frac{1}{\beta}\tan\left(\frac{\pi}{8}\right)\right)^{1/\alpha}\right)\right),$$

and

$$K\left(\frac{3}{4}\right) = -\frac{1}{\lambda}\log\left(1-\frac{2}{\pi}\arctan\left(\left(\frac{1}{\beta}\tan\left(\frac{3\pi}{8}\right)\right)^{1/\alpha}\right)\right).$$

The analytical tractability of the QF is a significant advantage for the NAT-E distribution. Beyond its utility for random number generation, it facilitates the direct calculation of skewness and kurtosis measures. For instance, in the light of Galton [8] and Moores [12], the quantile-based skewness and kurtosis of the NAT-E distribution are, respectively, defined as

$$S_k = \frac{K(6/8) - 2K(4/8) + K(2/8)}{K(6/8) - K(2/8)},$$

and

$$K_s = \frac{K(7/8) - K(5//8) + K(3/8) - K(1/8)}{K(6/8) - K(2/8)}.$$

Table 1 shows numerical computations of some measures of partition and shape.

Table 1: Quantile-based summary statistics for fixed $\lambda = 0.6$

Statistics	$(\alpha = 0.2, \beta = 0.3)$	$(\alpha = 0.5, \beta = 0.1)$	$(\alpha = 0.4, \beta = 0.5)$	$(\alpha = 0.3, \beta = 5)$
Lower quartile	3.4627	5.4919	0.0021	0.0006
Median	10.7858	8.4279	0.0191	0.0105
Upper quartile	18.1305	11.3658	0.1798	0.2073
Skewness	0.0015	0.0003	0.8087	0.9040
Kurtosis	1.1851	1.3694	6.3242	10.1369

Table 1 clearly explains the symmetric and asymmetric nature of the NAT-E distribution. The table also shows that the distribution accommodates both light-tailed and heavy-tailed behaviour.

4 Methods of Parameter Estimation

In this section, the unknown parameters of the NAT-E distributions are estimated using five different methods of parameter estimation, including the maximum likelihood, ordinary least squares, weighted least squares, maximum product spacing, and Anderson-Darling estimation methods. The parameters of the NAT-E distribution are denoted as $\xi = (\alpha, \beta, \lambda)$, and the corresponding estimates as $\hat{\xi} = (\hat{\alpha}, \hat{\beta}, \hat{\lambda})$. A brief mathematical representation of these methods is discussed in the following subsections.

4.1 Maximum likelihood estimation (MLE)

Suppose $x_1, x_2, \ldots, x_n$ are random samples following the NAT-E distribution, with PDF $f(x) = f(x; \xi)$ defined in Equation (3), and set $x = (x_1, x_2, \ldots, x_n)$, then the log-likelihood function is derived as

$$\begin{aligned} \ell_{\text{mle}}(x) &= \sum_{i=1}^{n} \log\left[f(x_i)\right] \\ &= \sum_{i=1}^{n} \log\left[\alpha\beta\lambda \frac{e^{-\lambda x_i}\left(\tan\left((\pi/2)e^{-\lambda x_i}\right)\right)^{-(\alpha-1)}}{\left(\sin\left((\pi/2)e^{-\lambda x_i}\right)\right)^{2}\left(1+\beta^{2}\left(\tan\left((\pi/2)e^{-\lambda x_i}\right)\right)^{-2\alpha}\right)}\right]. \end{aligned} \tag{5}$$

The estimates $\hat{\alpha}_{\text{mle}}$, $\hat{\beta}_{\text{mle}}$, and $\hat{\lambda}_{\text{mle}}$ of the parameters of the NAT-E distribution are obtained as the root of the system of equations

$$\frac{\partial \ell_{\text{mle}}(x)}{\partial \alpha} = 0, \quad \frac{\partial \ell_{\text{mle}}(x)}{\partial \beta} = 0, \quad \frac{\partial \ell_{\text{mle}}(x)}{\partial \lambda} = 0,$$

respectively.

4.2 Ordinary least squares estimation (OLSE)

Let $x_{(1)} < x_{(2)} < \cdots < x_{(n)}$ be an ordered sample associated with the CDF of the NAT-E distribution defined in Equation (2), the OLSE method seeks to minimize the objective function, which is the squared differences between the theoretical CDF and the empirical CDF function. Mathematically, it is presented as

$$\begin{aligned}\ell_{\text{olse}}(x) &= \sum_{i=1}^{n} \left[H(x_{(i)}) - E[H(x_{(i)})]\right]^2 \\ &= \sum_{i=1}^{n} \left[\frac{2}{\pi} \arctan\left(\beta\left(\tan\left(\frac{\pi}{2}(1-e^{-\lambda x_{(i)}})\right)\right)^{\alpha}\right) - \frac{i}{n+1}\right]^2.\end{aligned} \tag{6}$$

4.3 Weighted least squares estimation (WLSE)

An attempt to improve the efficiency of the OLSE method is to add a weight function to account for heteroscedasticity. The objective function of the WLSE is thus written as

$$\begin{aligned}\ell_{\text{wlse}}(x) &= \sum_{i=1}^{n} W_i \left[H(x_{(i)}) - E[H(x_{(i)})]\right]^2 \\ &= \sum_{i=1}^{n} \frac{(n+1)^2(n+2)}{[i(n-i+1)]} \left[\frac{2}{\pi} \arctan\left(\beta\left(\tan\left(\frac{\pi}{2}(1-e^{-\lambda x_{(i)}})\right)\right)^{\alpha}\right) - \frac{i}{n+1}\right]^2.\end{aligned} \tag{7}$$

4.4 Maximum product spacing estimation (MPSE)

Suppose the ordered sample $x_{(1)} < x_{(2)} < \cdots < x_{(n)}$ follows the NAT-E distribution with CDF defined in Equation (2). The idea of the MPSE method is such that the differences between the values of the distribution function at consecutive observed values should be identically distributed. The MPSE method maximizes the objective function

$$\ell_{\text{mpse}}(x) = \frac{1}{n+1} \sum_{i=1}^{n+1} \log\left[H(x_{(i)}) - H(x_{(i-1)})\right]. \tag{8}$$

4.5 Anderson–Darling estimation (ADE)

Given the CDF in Equation (2), the parameter estimates of the NAT-E distribution are obtained through the ADE method by minimizing the objective function

$$\ell_{\text{ade}}(x) = -n - \sum_{i=1}^{n} \frac{2i-1}{n} \left\{ \log[H(x_{(i)})] + \log\left[1 - H(x_{(n-i+1)}; \xi)\right] \right\}. \tag{9}$$

5 Simulation Experiment

This section investigates the asymptotic behaviour of the unknown parameters of the NAT-E distribution using the different methods of estimation via a Monte Carlo simulation study. The experiment considers two sets of true parameter values: $(\alpha_0 = 0.6, \beta_0 = 0.8, \lambda_0 = 0.5)$ and $(\alpha_0 = 0.9, \beta_0 = 0.4, \lambda_0 = 0.3)$. Based on these values, random samples of sizes $n = 25, 50, 100, 200$, and 500 are generated from the NAT-E distribution using the QF defined in Equation (4). The step-by-step procedure for achieving this task is given as follows:

Step 1: Define the number of Monte Carlo simulations ($N = 1000$);

Step 2: Generate a random sample of size n;

Step 3: Estimate the sample using the different methods of estimation;

Step 4: Repeat steps 2-3, N-times, and compute the quantities

(i) Mean absolute error (MAE) $= \frac{1}{N} \sum_{i=1}^{N} |\hat{\xi}_i - \xi_0|$

(ii) Root mean square error (RMSE) $= \sqrt{\frac{1}{N} \sum_{i=1}^{N} (\hat{\xi}_i - \xi_0)^2}$.

Tables 2 and 3 present the simulation results of the MAE and the RMSE of the parameters of NAT-E distribution.

Table 2: Simulation result of the MAE and RMSE for ($\alpha = 0.6$, $\beta = 0.8$, $\lambda = 0.5$)

		MAE					RMSE				
Parameter	n	MLE	OLSE	WLSE	MPSE	ADE	MLE	OLSE	WLSE	MPSE	ADE
α	25	0.1457	0.1614	0.1545	0.1749	0.1484	0.1973	0.2055	0.1991	0.2379	0.1959
	50	0.1007	0.1130	0.1072	0.1115	0.1034	0.1319	0.1450	0.1385	0.1486	0.1338
	100	0.0682	0.0767	0.0711	0.0729	0.0701	0.0862	0.0969	0.0892	0.0943	0.0882
	200	0.0475	0.0545	0.0498	0.0494	0.0490	0.0595	0.0686	0.0622	0.0623	0.0615
	500	0.0301	0.0343	0.0309	0.0307	0.0309	0.0386	0.0436	0.0395	0.0393	0.0394
β	25	0.3551	0.6339	0.5518	0.3447	0.4106	0.5453	2.5301	3.1290	0.5222	0.8270
	50	0.2415	0.2843	0.2627	0.2337	0.2521	0.3392	0.4836	0.3710	0.3152	0.3588
	100	0.1556	0.1738	0.1623	0.1523	0.1589	0.2010	0.2304	0.2116	0.1949	0.2072
	200	0.1056	0.1211	0.1106	0.1050	0.1095	0.1357	0.1558	0.1424	0.1345	0.1411
	500	0.0673	0.0739	0.0682	0.0669	0.0681	0.0846	0.0945	0.0866	0.0841	0.0865
λ	25	0.1972	0.2668	0.2471	0.1802	0.2141	0.2756	0.4003	0.3654	0.2467	0.2933
	50	0.1369	0.1707	0.1564	0.1304	0.1459	0.1793	0.2278	0.2039	0.1714	0.1897
	100	0.0910	0.1104	0.0986	0.0885	0.0959	0.1143	0.1393	0.1239	0.1114	0.1205
	200	0.0633	0.0775	0.0685	0.0622	0.0667	0.0811	0.0980	0.0871	0.0796	0.0852
	500	0.0419	0.0490	0.0437	0.0416	0.0434	0.0526	0.0620	0.0548	0.0520	0.0545

Table 3: Simulation result of the MAE and RMSE for ($\alpha = 0.9$, $\beta = 0.4$, $\lambda = 0.3$)

		AB					RMSE				
Parameter	n	MLE	OLSE	WLSE	MPSE	ADE	MLE	OLSE	WLSE	MPSE	ADE
α	25	0.2958	0.3678	0.3427	0.3595	0.3123	0.4013	0.4696	0.4373	0.4915	0.4081
	50	0.2088	0.2676	0.2360	0.2341	0.2246	0.2762	0.3362	0.3015	0.3145	0.2911
	100	0.1457	0.1854	0.1594	0.1575	0.1548	0.1890	0.2339	0.2028	0.2076	0.1980
	200	0.1015	0.1290	0.1097	0.1051	0.1084	0.1298	0.1657	0.1409	0.1357	0.1386
	500	0.0626	0.0803	0.0680	0.0633	0.0676	0.0788	0.1017	0.0850	0.0808	0.0845
β	25	0.3400	2.4601	2.0669	0.3255	1.0279	0.8371	11.2617	11.2561	0.7907	7.7592
	50	0.1974	0.4521	0.3798	0.1878	0.2626	0.3551	2.4444	3.2991	0.3216	1.3219
	100	0.1168	0.1507	0.1292	0.1146	0.1229	0.1725	0.2233	0.1841	0.1577	0.1694
	200	0.0752	0.0932	0.0809	0.0747	0.0793	0.1067	0.1369	0.1162	0.1059	0.1137
	500	0.0457	0.0550	0.0478	0.0455	0.0475	0.0585	0.0718	0.0615	0.0581	0.0611
λ	25	0.1317	0.2604	0.2322	0.1106	0.1716	0.2029	0.5099	0.5276	0.1518	0.2916
	50	0.0956	0.1412	0.1189	0.0836	0.1082	0.1377	0.1954	0.1584	0.1052	0.1421
	100	0.0651	0.0906	0.0760	0.0613	0.0720	0.0843	0.1194	0.0982	0.0780	0.0936
	200	0.0488	0.0621	0.0533	0.0466	0.0524	0.0626	0.0814	0.0687	0.0593	0.0676
	500	0.0293	0.0382	0.0320	0.0286	0.0318	0.0368	0.0490	0.0404	0.0359	0.0402

An examination of Tables 2 and 3 shows that both the MAE and the RMSE decline monotonically as the sample size n increases for all estimation methods. This pattern is consistent with the property of consistency: as n grows, the estimators converge in probability to the true parameter values. Regarding relative performance, the MLE yields the smallest bias and RMSE for α, indicating superior accuracy for this parameter. In contrast, the MPSE outperforms the other methods for β and λ, producing lower bias and RMSE across the considered sample sizes. Thus, while all methods are consistent, their finite-sample efficiency varies by parameter. MLE is preferred for estimating α, whereas MPSE is more effective for β and λ.

6 Practical Data Applications

This section utilizes three real-world datasets to illustrate the usefulness and potential applicability of the proposed NAT and NAT-E distributions. The first dataset is a unit-interval dataset representing trade share, available as an online complement to [16]. [4] has used the dataset to validate the performance of the power continuous Bernoulli distribution. The second and third datasets, respectively, comprise the failure times of 50 components and the exceedances of flood peaks (in m3/s) of the Wheaton River near Carcross in Yukon Territory, Canada, reported in [2]. The datasets are given below.

Dataset I (Trade Share Data): 0.140501976, 0.156622976, 0.157703221, 0.160405084, 0.160815045, 0.22145839, 0.299405932, 0.31307286, 0.324612707, 0.324745566, 0.329479247, 0.330021679, 0.337879002, 0.339706242, 0.352317631, 0.358856708, 0.393250912, 0.41760394, 0.425837249, 0.43557933, 0.442142904, 0.444374621, 0.450546652, 0.4557693, 0.46834656, 0.473254889, 0.484600782, 0.488949597, 0.509590268, 0.517664552, 0.527773321, 0.534684658, 0.543337107, 0.544243515, 0.550812602, 0.552722335, 0.56064254, 0.56074965, 0.567130983, 0.575274825, 0.582814276, 0.603035331, 0.605031252, 0.613616884, 0.626079738, 0.639484167, 0.646913528, 0.651203632, 0.681555152, 0.699432909, 0.704819918, 0.729232311, 0.742971599, 0.745497823, 0.779847085, 0.798375845, 0.814710021, 0.822956383, 0.830238342, 0.834204197, 0.979355395.

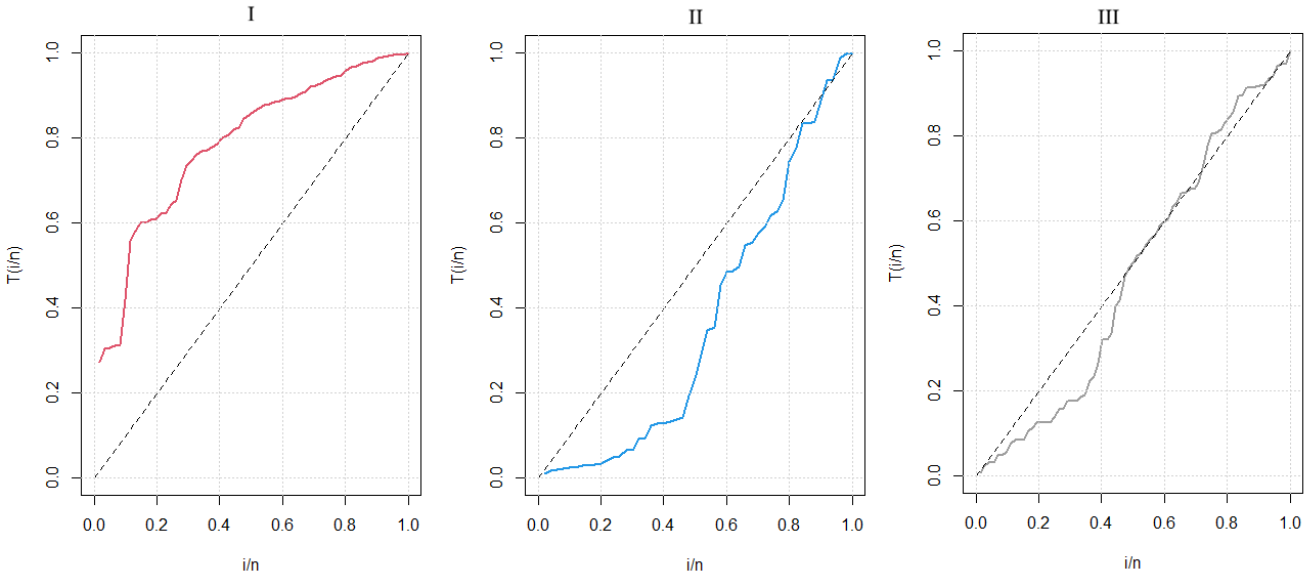
Dataset II (Failure Time Data): 0.036, 0.058, 0.061, 0.074, 0.078, 0.086, 0.102, 0.103, 0.114, 0.116, 0.148, 0.183, 0.192, 0.254, 0.262, 0.379, 0.381, 0.538, 0.570, 0.574, 0.590, 0.618, 0.645, 0.961, 1.228, 1.600, 2.006, 2.054, 2.804, 3.058, 3.076, 3.147, 3.625, 3.704, 3.931, 4.073, 4.393, 4.534, 4.893, 6.274, 6.816, 7.896, 7.904, 8.022, 9.337, 10.940, 11.020, 13.880, 14.730, 15.080.

Dataset III (Exceedances of Flood Peaks Data): 1.7, 2.2, 14.4, 1.1, 0.4, 20.6, 5.3, 0.7, 1.9, 13, 12, 9.3, 1.4, 18.7, 8.5, 25.5, 11.6, 14.1, 22.1, 1.1, 2.5, 14.4, 1.7, 37.6, 0.6, 2.2, 39, 0.3, 15, 11, 7.3, 22.9, 0.1, 1.7, 1.1, 0.6, 9, 1.7, 7, 20.1, 0.4, 2.8, 14.1, 9.9, 10.4, 10.7, 30, 3.6, 5.6, 30.8, 13.3, 4.2, 25.5, 3.4, 11.9, 21.5, 27.6, 36.4, 2.7, 64, 1.5, 2.5, 27.4, 1, 27.1, 20.2, 16.8, 5.3, 9.7, 27.5, 2.5, 27.

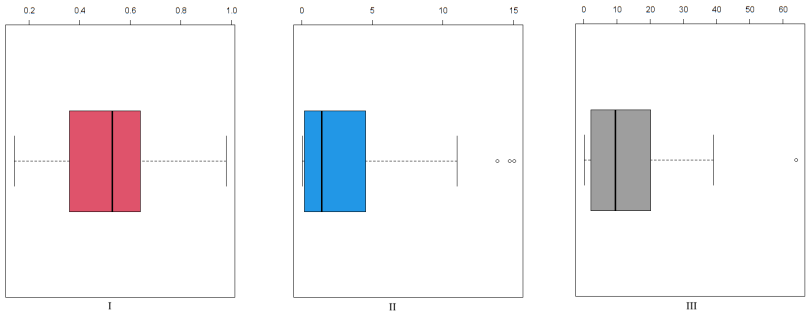
An exploratory data analysis showing the summary statistics and graphical representations of the datasets are displayed in Table 4 and Figure 5, respectively.

Table 4: The summary statistics for the datasets

Dataset	Min.	Mean	Median	Variance	Skewness	Kurtosis	Max.
I	0.1405	0.5142	0.5278	0.0375	0.0060	2.5526	0.9794
II	0.0360	3.3430	1.4140	17.4848	1.4167	4.0846	15.0800
III	0.1000	12.2040	9.5000	151.2215	1.4725	5.8895	64.0000



(a) The TTT curve for each dataset



(b) The Boxplot for each dataset

Figure 5: Graphical representation showing the TTT curve and boxplot for each dataset.

A careful examination of Table 4 reveals that the first dataset is approximately symmetric, while the second and third datasets are right-skewed. On the other hand, the total test time (TTT) curve in Figure 5 indicates that the three datasets exhibit increasing, decreasing, and bathtub-shaped hazard-rate

properties, respectively. Also, the boxplot shows that the first dataset is approximately symmetric and free of outliers, whereas the second and third datasets are right-skewed and contain outliers.

Furthermore, the NAT distribution, together with standard benchmark unit distributions such as the beta, Kumaraswamy, Sine Marshall-Olkin Topp-Leone (SMOTL) introduced by [14], Marshall-Olkin Topp-Leone (MOTL) developed by [15], Unit-Weibull (UW) reported in [10], Unit-Gompertz (UG) studied by [9], and Unit-logistic (UL) due to [11], are used to fit the first dataset. Also, the applicability of the NAT-E distribution in fitting the second and third datasets is compared with the fit of some well-known distributions, including the exponentiated Weibull (EW) reported in [13], Weibull, gamma, weighted harmonic sine exponential (WHSE) developed by [5], exponentiated exponential (EE) examined in [6], sine exponential (SE) introduced by [7], and the classical exponential distribution.

The comparison of results obtained from the fitting are based on the maximized log-likelihood (LogL), Akaike information criterion (AIC), Kolmogorov-Smirnov (K-S), Cramér-von Mises (W^*), and Anderson Darling (A^*) test statistics, with their associated p-values. The results are shown in Tables 5, 6, and 7.

Table 5: Summary statistics for Dataset I (Trade Share Data)

Distribution	Estimates (Std. error)	LogL	AIC	K-S (p-value)	W^* (p-value)	A^* (p-value)
NAT	$\hat{\alpha} = 2.0144(0.2332)$ $\hat{\beta} = 0.9049(0.1624)$	14.6643	-25.3287	0.0465 (0.9986)	0.0241 (0.9919)	0.2421 (0.9744)
SMOTL	$\hat{\alpha} = 2.2453(0.9307)$ $\hat{\lambda} = 2.5193(0.6977)$	11.4619	-18.9238	0.0611 (0.9662)	0.0441 (0.9128)	0.4888 (0.7575)
MOTL	$\hat{\alpha} = 0.6631(0.2825)$ $\hat{\lambda} = 3.3516(0.7565)$	14.3606	-24.7211	0.0567 (0.9831)	0.0447 (0.9091)	0.3925 (0.8557)
UW	$\hat{\alpha} = 1.3395(0.1726)$ $\hat{\beta} = 1.7345(0.1695)$	14.2436	-24.4872	0.0682 (0.9210)	0.0617 (0.8049)	0.5034 (0.7427)
UG	$\hat{\alpha} = 0.6162(0.2659)$ $\hat{\beta} = 1.0921(0.2471)$	10.8759	-17.7518	0.1098 (0.4235)	0.2076 (0.2535)	1.4468 (0.1897)
UL	$\hat{\beta} = 1.9291(0.2079)$ $\hat{\mu} = 0.5157(0.0285)$	14.5826	-25.1651	0.0483 (0.9976)	0.0280 (0.9830)	0.2641 (0.9623)
Beta	$\hat{\alpha} = 2.7940(0.4880)$ $\hat{\beta} = 2.6038(2.6038)$	13.9561	-23.9121	0.0618 (0.9629)	0.0470 (0.8958)	0.3759 (0.8717)
Kumaraswamy	$\hat{\alpha} = 2.3301(0.3056)$ $\hat{\beta} = 2.7638(0.5553)$	13.6251	-23.2503	0.0689 (0.9143)	0.0557 (0.8423)	0.4115 (0.8367)

Table 6: Summary statistics for Dataset II (Failure Time Data)

Distribution	Estimates (Std. error)	LogL	AIC	K-S (p-value)	W^* (p-value)	A^* (p-value)
NAT-E	$\hat{\alpha} = 0.6118(0.1000)$ $\hat{\beta} = 1.2823(0.4312)$ $\hat{\lambda} = 0.3423(0.1049)$	-100.5816	207.1631	0.0973 (0.6949)	0.0885 (0.6462)	0.6328 (0.6167)
EW	$\hat{\alpha} = 0.7833(1.4769)$ $\hat{\beta} = 0.3843(1.1165)$ $\hat{\lambda} = 0.7713(0.9504)$	-102.3563	210.7125	0.1333 (0.3084)	0.1517 (0.3853)	0.9466 (0.3860)
Weibull	$\hat{\alpha} = 0.6610(0.0748)$ $\hat{\beta} = 2.5289(0.5712)$	-102.3643	208.7287	0.1269 (0.3656)	0.1552 (0.3750)	0.9628 (0.3769)
Gamma	$\hat{\alpha} = 0.5461(0.0909)$ $\hat{\lambda} = 6.1182(1.5502)$	-102.4367	208.8735	0.1425 (0.2385)	0.1527 (0.3825)	0.9555 (0.3810)
WHSE	$\hat{\alpha} = 0.9175(0.5242)$ $\hat{\lambda} = 0.2920(0.0627)$	-110.3310	224.6621	0.2832 (0.0005)	0.8317 (0.0060)	6.7896 (0.0005)
EE	$\hat{\lambda} = 5.1498(1.1448)$ $\hat{\theta} = 0.5367(0.0901)$	-102.3725	208.7449	0.1428 (0.2359)	0.1500 (0.3905)	0.9425 (0.3884)
SE	$\hat{\lambda} = 0.1612(0.0218)$	-112.4518	226.9036	0.3055 (0.0001)	0.9853 (0.0025)	8.2740 (0.00009)
Exponential	$\hat{\lambda} = 0.2991(0.0423)$	-110.3428	222.6857	0.2845 (0.0004)	0.8401 (0.0056)	6.8572 (0.0004)

Table 7: Summary statistics for Dataset III (Exceedances of Flood Peaks Data)

Distribution	Estimates (Std. error)	LogL	AIC	K-S (p-value)	W^* (p-value)	A^* (p-value)
NAT-E	$\hat{\alpha} = 0.7729(0.1209)$ $\hat{\beta} = 0.8169(0.2515)$ $\hat{\lambda} = 0.1057(0.0275)$	-250.4369	506.8738	0.0928 (0.5646)	0.0839 (0.6707)	0.5266 (0.7192)
EW	$\hat{\alpha} = 0.5180(0.1998)$ $\hat{\beta} = 0.0157(0.0226)$ $\hat{\lambda} = 1.3874(0.3679)$	-251.0251	508.0502	0.1074 (0.3778)	0.1055 (0.5600)	0.6438 (0.6070)
Weibull	$\hat{\alpha} = 0.8996(0.0854)$ $\hat{\beta} = 11.6028(1.5986)$	-251.4989	506.9978	0.1043 (0.4143)	0.1488 (0.3939)	0.8415 (0.4516)
Gamma	$\hat{\alpha} = 0.8377(0.1209)$ $\hat{\lambda} = 14.5583(2.8127)$	-251.3444	506.6888	0.1024 (0.4367)	0.1336 (0.4444)	0.7635 (0.5076)
WHSE	$\hat{\alpha} = 1.6018(0.8264)$ $\hat{\lambda} = 0.0969(0.0204)$	-251.8427	507.6854	0.1507 (0.0762)	0.2432 (0.1974)	1.5765 (0.1593)
EE	$\hat{\lambda} = 13.8020(2.2301)$ $\hat{\theta} = 0.8286(0.1231)$	-251.2936	506.5871	0.1017 (0.4459)	0.1301 (0.4571)	0.7453 (0.5217)
SE	$\hat{\lambda} = 0.0450(0.0050)$	-252.9233	507.8466	0.1622 (0.0454)	0.2958 (0.1389)	1.9826 (0.0941)
Exponential	$\hat{\lambda} = 0.0819(0.0097)$	-252.1280	506.2559	0.1422 (0.1087)	0.2307 (0.2153)	1.4586 (0.1867)

In practice, the most appropriate model in practical data fitting is associated with the model having the maximized log-likelihood value $LogL$ and the smallest value in terms of the AIC, K-S, W^*, and A^*. Consequently, the results in Tables 5, 6, and 7 reveal that the proposed NAT and NAT-E distributions outperformed the competing distributions in fitting the three datasets under study. However, based on AIC, the gamma, exponential, and EE distributions are preferred for the third dataset, as the criterion penalizes complex models.

Furthermore, this claim is supported by graphical goodness-of-fit tests, such as probability-probability (P-P) plots. The plots are displayed in Figures 6, 7, and 8.

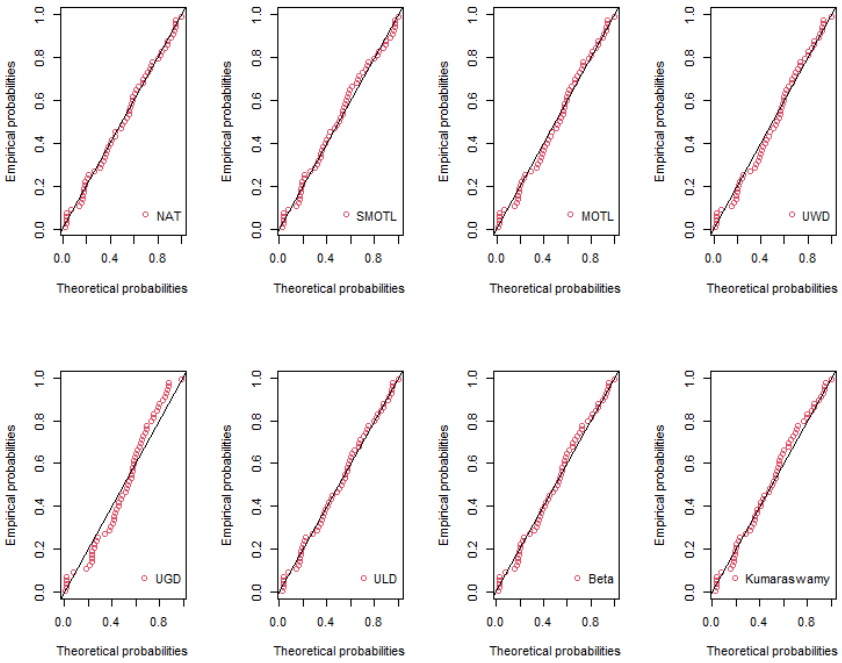


Figure 6: The P-P plot for Dataset I (Trade Share Data).

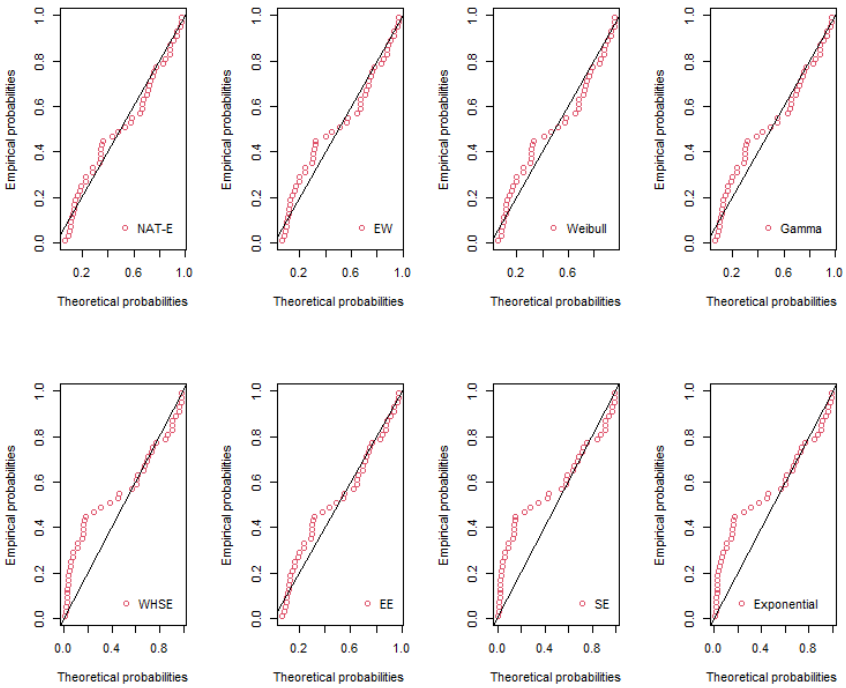


Figure 7: The P-P plot for Dataset II (Failure Time Data).

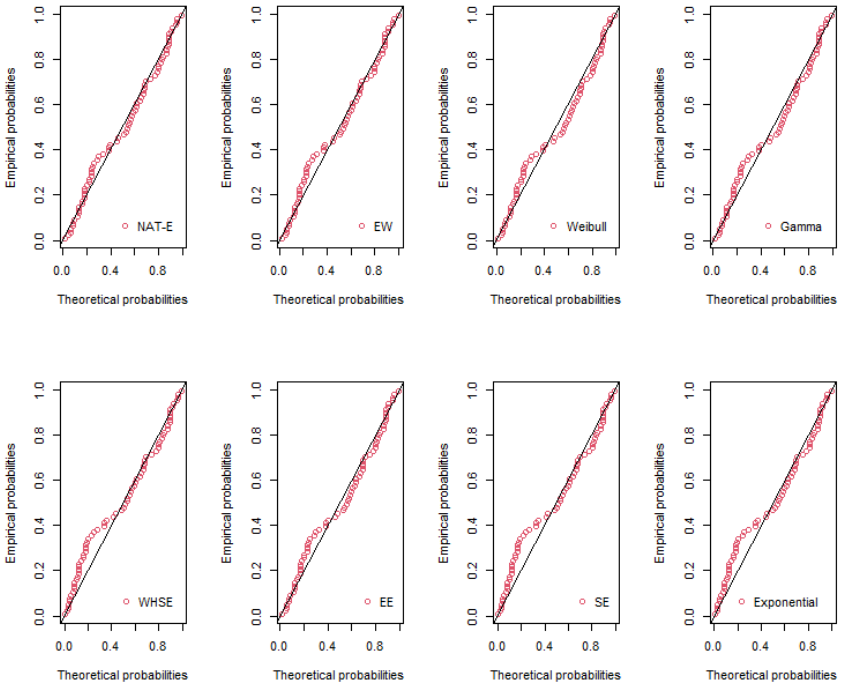


Figure 8: The P-P plot for Dataset III (Exceedances of Flood Peaks Data).

7 Conclusion

In this article, we have introduced two new distributions: the NAT distribution and its three-parameter lifetime counterpart, the NAT-E distribution. We demonstrated that both distributions possess analytically tractable probabilistic functions, including closed-form expressions for their CDFs, PDFs, and QFs. Our analysis revealed that these distributions offer significant structural flexibility, accommodating a wide range of shapes, including symmetric and asymmetric properties. The simulation results show that all estimation methods for the NAT-E distribution are consistent: bias and RMSE decrease toward zero as the sample size n increases. In finite samples, however, performance varies by parameter. MLE yields the lowest bias and RMSE for α, indicating higher precision and efficiency for that parameter. For β and λ, MPSE outperforms the other methods on both metrics. Finally, empirical results from three real-world datasets confirmed that the proposed models can outperform established benchmarks in the literature, making them robust tools for data modeling.

Funding

No funding was received for this study.

Conflict of Interest

Authors declare that they have no conflicts of interest with respect to this study.

Acknowledgement

We thank the anonymous referee(s) for valuable comments on an earlier version of this paper.

References

[1] Afuecheta, E., Okorie, I. E., Jallow, H., & Nadarajah, S. (2025). A review of unit continuous probability distributions. *AIMS Mathematics, 10*(11), 25939–26057.

[2] Arshad, M. Z., Iqbal, M. Z., & Al Mutairi, A. (2021). A comprehensive review of datasets for statistical research in probability and quality control. *Journal of Mathematical and Computational Science, 11*(3), 3663–3728. https://doi.org/10.28919/jmcs/5692

[3] Chesneau, C. (2026). Two new and simple ideas of one-parameter trigonometric unit distributions. *Advances in Mathematics: Scientific Journal, 15*(2), 191–206.

[4] Chesneau, C., & Opone, F. C. (2022). The power continuous Bernoulli distributions: Theory and applications. *Reliability: Theory & Applications, 17*(4(71)), 232–248.

[5] Chesneau, C., & Opone, F. C. (2023). Exploring the weighted harmonic mean transformation to generate new probability distributions. *International Journal of Open Problems in Computer Science and Mathematics, 16*(4).

[6] Gupta, R. D., & Kundu, D. (2001). Exponentiated exponential family: An alternative to gamma and Weibull distributions. *Biometrical Journal, 43*(1), 117–130. https://doi.org/10.1002/1521-4036(200102)43:1<117::AID-BIMJ117>3.0.CO;2-R

[7] Isa, A. M., Sule, O. B., Ali, B. A., Akeem, A. A., & Ibrahim, I. I. (2022). Sine-exponential distribution: Its mathematical properties and application to real dataset. *UMYU Scientifica, 1*(1), 127–131.

[8] Kenney, J. F., & Keeping, E. S. (1962). *Mathematics of statistics* (3rd ed., Pt. 1). Van Nostrand.

[9] Mazucheli, J., Menezes, A. F. B., & Dey, S. (2019). Unit-Gompertz distribution with applications. *Statistica, 79*(1), 25–43.

[10] Mazucheli, J., Menezes, A. F. B., Fernandes, L. B., de Oliveira, R. P., & Ghitany, M. E. (2020). The unit-Weibull distribution as an alternative to the Kumaraswamy distribution for the modeling of quantiles conditional on covariates. *Journal of Applied Statistics, 47*(6), 954–974. https://doi.org/10.1080/02664763.2019.1659130

[11] Menezes, A. F. B., Mazucheli, J., & Dey, S. (2018). The unit-logistic distribution: Different methods of estimation. *Pesquisa Operacional, 38*(3), 555–578.

[12] Moors, J. J. A. (1988). A quantile alternative for kurtosis. *The Statistician, 37*(1), 25-32. https://doi.org/10.2307/2348376

[13] Mudholkar, G. S., & Hutson, A. D. (1996). The exponentiated Weibull family: Some properties and a flood data application. *Communications in Statistics – Theory and Methods, 25*(12), 3059–3083. https://doi.org/10.1080/03610929608831886

[14] Ogumeyo, S. A., Opone, F. C., Abubakari, A. G., & Ehiwario, J. C. (2024). A bounded lifetime distribution specified by a trigonometric function: Properties, regression model, and applications. *International Journal of Mathematics and Mathematical Sciences, 2024*(1), 5583105. https://doi.org/10.1155/2024/5583105

[15] Opone, F. C., & Iwerumor, B. N. (2021). A new Marshall-Olkin extended family of distributions with bounded support. *Gazi University Journal of Science, 34*(3), 899–914.

[16] Stock, J. H., & Watson, M. W. (2007). *Introduction to econometrics* (2nd ed.). Addison Wesley. Dataset available online: https://rdrr.io/cran/AER/man/GrowthSW.html

This is an open access article distributed under the terms of the Creative Commons Attribution License (http://creativecommons.org/licenses/by/4.0/), which permits unrestricted, use, distribution and reproduction in any medium, or format for any purpose, even commercially provided the work is properly cited.